TRANSFER LEARNING FOR ANOMALY DETECTION USING BEARINGS' VIBRATION SIGNALS

Diego Nieves Avendano*, Dirk Deschrijver, Sofie Van Hoecke,
Ghent University - imec
Ghent, Belgium
Corresponding author* {diego.nievesavendano@ugent.be}

ABSTRACT

Context. Predictive maintenance is becoming increasingly important in the industry. Despite considerable advances in data collection and data-driven models, there are still limitations when deploying models in practice. One of the main limitations is the large datasets required to train these models. As a potential solution, transfer learning can be used to reuse knowledge acquired from large datasets for similar tasks under different conditions. This paper investigates the transferability for the specific scenario of anomaly detection, an unsupervised learning task with heavily imbalanced label distribution.

Methods. This paper uses a dataset generated from a bearing test platform in which bearings are run until failure under different operating conditions. A lightweight deep learning model, MobileNetV2, is employed to create a baseline model capable of detecting anomalies for a specific operating condition. The model is then adapted using transfer learning to accurately identify anomalies under new operating conditions with limited data.

Results. The results show that the data for new conditions is insufficient to train an adequate model, and that this limitation is overcome using transfer learning. The adapted models can to detect anomalies prior to the expert's knowledge reference value. Although this shows that transfer learning can detect anomalies earlier, the results need to be evaluated with care to avoid false positives.

Conclusion. While anomaly detection aims to identify changes in feature distributions, transfer learning aims to align different feature distributions. Transfer learning for unsupervised learning has been rarely explored, and to the best of our knowledge, this is one of the few works addressing it in the context of predictive maintenance for anomaly detection.

1. INTRODUCTION

Predictive maintenance (PdM) models of mechanical components are a key aspect for Prognostics and Health Management (PHM) within the industry. Accurate PdM models contribute to improvements in terms of quality, safety, maintenance scheduling, and cost reduction. Anomaly detection (AD) most commonly refers to the unsupervised task of detecting events that deviate from normal operating conditions. This paper examines the use of artificial neural networks and transfer learning on vibration data from bearings under different operating conditions (speed changes) for the purpose anomaly detection. The methodology is evaluated using the Smart Maintenance Living Lab (SMLL) dataset by Flanders Make and imec.[1]

While deep learning techniques have been successfully used for fault identification and classification, the application of transfer learning (TL) in anomaly detection has been limited so far. This is not surprising given that AD is an inherently challenging task, due to the frequent lack of ground truth and being an imbalanced unsupervised task. In addition, AD is on its own the task of detecting shifts in the data features which correspond to unexpected behavior, while TL is the task of consolidating data with different feature distributions as normal behaviors. In other words, a straightforward AD approach would label samples coming from new domains as anomalous. Therefore the challenge at hand consists in finding a representation that maps abundant information from the source to the sparse target domain for improved anomaly identification in both domains.

This paper is divided as follows: Section 2 reviews existing literature related to PdM tasks using deep learning and transfer learning techniques, with a special focus on fault classification and anomaly detection. Section 3 introduces the SMLL dataset. Section 4 outlines the methodology, which consists of the data processing, the details on the baseline model and how the model is adapted to the different operational conditions. Section 5 presents the results and discussion of the results obtained in the baseline and the transfer learning generalization performance. Section 6 proposes future research work based on the insights gained. Finally, section 7 presents the conclusion.

2. RELATED WORK

Physics based and statistical models have previously been used for the analysis of vibration signals of bearings for tasks such as detecting degradation onset; fault detection and classification; and estimation remaining useful life (RUL).[2] However, in recent years, deep learning techniques have gained attention due to their improved performance, ability to discover features from raw, or lightly processed, sensor data, capability to model complex processes without prior domain knowledge, and requiring minimal assumptions about feature distributions.[2,3] Moreover, deep learning models offer advantages in the context of transfer learning owing to their inherent ability of learning complex representations that can be generalized across different contexts. In addition, they possess high transferability even across considerably different tasks, and have been proven to boost generalization on new tasks when starting from a pre-trained model.[4]

This section starts by presenting an overview of the deep learning literature concerning general PdM tasks. Subsequently, it presents a literature review of transfer learning in the context of PdM. Finally, it discusses the advantages of using lightweight deep learning models.

2.1. Deep Learning in PdM Tasks

In order to solve PdM tasks, deep learning techniques, specifically Artificial Neural Networks (ANNs), have been employed to analyze raw time signals in order to predict different fault types of some of the most popular bearing datasets such as the Case Western Reserve University (CWRU) and the Intelligent Maintenance System (IMS) Bearing Dataset.[5] However, using dense layers over temporal data is only possible with relatively small time windows as the dimensionality of the network increases drastically with high sampling rates. To solve this limitation, different approaches that reduce the signal complexity can be used, such as representation learning or transformations of the vibration signal.

Representation learning techniques, like dictionary learning, allow learning complex signals in reduced spaces via linear combinations of prototype signals called atoms. These sparse dictionary learning technique has been used in combination with data augmentation techniques for the diagnosis of planetary bearings.[6] Alternatively, transforming vibration data from the time domain into the frequency domain allows for compact inputs and can prevent the neural networks from being overparametrized. Moreover, spectral representations remove the need of correctly detecting and aligning the peaks of the carrier signal as well as the characteristic frequency components, which would otherwise require the alignment to extract the correct features in the input layer of the neural network. Spectrogram representations have been used with feed-forward ANNs,[7] self organizing maps,[8] and other deep learning architectures.[9]

Given the time and frequency relations between adjacent samples, Convolutional Neural Networks (CNN) are an evident model choice. CNNs are characterized for their ability of discovering structural information in the data, in addition to being more parameter efficient than ANNs. CNN architectures have been used over temporal data in many forms such as the raw vibration signals,[10–12] as well as filtered and pre-processed signals.[13] In some cases, time series can be treated as a special case of two-dimensional convolutions, either by splitting a time window into segments and using each segment as a separate channel,[14] or by rearranging the segments and processing them as two-dimensional images.[5, 15] However, it is important to notice that these approaches can be computationally expensive as machines operate at high frequency that would need to be represented in large input vectors in order to be meaningful. Furthermore, the temporal representation is sensible to the location of the peaks of the carrier signal. This limitation can be be alleviated by using pooling operators to induce translation invariance, but this is only possible if there is a sufficient amount of pooling layers which may come at the expense of increased model complexity.

In contrast, using the spectral representation there is no limitation concerning the location of the carrier and characteristic frequency components. Other two dimensional representations that have been used are the frequency spectrogram over time.[16–18] The representation used in their research aligns with the one selected in this research. Other frequency-time representations such as the wavelet decomposition have also proven succesful.[19–22] Finally, architectures focused on temporal relations, such as Recurrent Neural Networks (RNNs) and Long short-term Memory (LSTM), are also used due to their inherent capacity of learning from data with long range temporal dependencies.[23–27] These techniques can once again be applied over temporal data, or temporal-frequency decomposition. In general, the literature review points to a preference towards frequency representations as they reduce the model's complexity and are able to preserve the important information for correct diagnosis.

In specific PdM tasks, CNNs have been investigated for the creation of health indexes, which are unit-less metrics that assist in condition monitoring,[28,29] estimating remaining useful life,[14,30,31] fault classification,[30,32] as well as anomaly detection.[24,31] Furthermore, RNNs and LSTMs have been investigated for remaining useful life estimation,[23,26,33] fault classification,[25] as well as anomaly detection.[24,27] It is clear that field has considerable amount of interest which has grown rapidly in recent years, more extensive reviews can be found in recent field surveys.[9]

2.2. Transfer Learning in PdM Tasks

Transfer learning addresses a range of problems in which the objective is reusing previously acquired knowledge for similar tasks. The TL problem can be phrased as follows: (i) given a group of Domains $\mathscr{D}$, each domain contains a dataset with a given set of features; (ii) the features in each domain measure the same properties or similar ones, but the distributions across domains differ; and (iii) TL finds a way to leverage the common information across domains to improve results on the task for any given domain. Most commonly, TL is viewed as a problem in which for a first domain there is a considerable amount of (high quality) data and the knowledge of this domain wants to be applied on a new domain, where there is a limited amount of data, and sometimes of lower quality. In other cases it can be seen as reusing a model trained to solve a certain task (e.g. image recognition) in order to solve a secondary task (e.g. semantic segmentation).

Two of common approaches in transfer learning for pre-trained models are stacking and fine-tuning. In both approaches, a neural network is trained with a large amount of high quality data from the source domain. Afterwards, this trained model is adapted for a secondary task either by stacking or fine-tuning. Stacking is an approach in which a mid-layer output of the model is used as the input of a new machine learning model. In fine-tuning the baseline model is further trained using the data from the new domain while restricting weight adaptation to the last few layers. Additionally, a third scenario exists, where a small number of layers are appended after embedding extraction. These, combined with a subset of the baseline model's layers, are then fine-tuned.

Large deep learning models, such as ResNet[34] and InceptionV3,[35] were originally developed for image classification tasks and trained on the Imagenet dataset,[36] which consists of real-world object images; however, the trained versions of these models have been reused for different tasks with different data representations. For example, fault classification of wind turbine gearboxes using wavelet representation as inputs and the pre-trained ResNet as feature map extraction;[32] fault detection in photovoltaic plants using thermal images and the pre-trained ResNet;[37] and wear estimation of cutting tools based on image inputs using pre-trained models such as ResNet, InceptionV3 and AlexNet as basis for a fine-tuning approach.[30] It is important to consider the validity of pre-trained weights in these approaches, as they have been trained to recognize objects in real-life images. However, this may not directly translate to representations of spectrograms or other types of images, such as the physical condition of mechanical components.

Regardless of whether the use of real-life image trained networks is a valid approach, a more common problem is the transfer learning task within two predictive maintenance tasks. This shift can occur in cases where the source and target correspond to similar components with different specifications;[10] the analysis of different fault types;[38] or discrepancies in data distributions of the same mechanical component due to large heterogeneity.[27,39] Overall, the coverage of studies on transferal with the end goal of anomaly detection has been limited.

To the best of our knowledge, there are limited studies of anomaly detection research in the context of transfer learning (AD-TL). One such work is presented by Michau et al.,[40] where they detedct anomalies in simulated engines operating under different conditions from the Turbofan jet engine dataset as well as faulty bearings from the CWRU dataset. Their approach consists of input alignment using adversarial deep learning. The main advantage of their method is the possibility of doing the transferal in an unsupervised way, removing the need of collecting labels in the target. Their results point to an accuracy of up to 100%, however, the authors specify that this is only achievable if the number of source and target data points is the same. In many transfer scenarios, included the presented in this paper, there is a considerable imbalance between source and target domains.

Another example of AD-TL uses Siamese networks in image recognition tasks.[41] Their research is conducted on hyperspectral images, and the end goal is to detect pixel anomalies over satellite pictures. To achieve this, the deep learning model is trained in a self-supervised approach in which random pixels are evaluated as originating from the same picture. In order to detect anomalies, the pixels of a figure are compared against their neighbors and a likelihood score is obtained through the Siamese network. This approach is not applicable to the presented research as spectrograms are not translation invariant as real world images are.

Compared to previous work, the task of AD-TL in the context of PdM presents the following differences: Due to the costs associated in generating samples, (i) source datasets tend to be considerably smaller than those seen in other domains such as image classification; and (ii) the ratio of samples between source and target domain is heavily imbalanced. Traditional TL benchmarks have more balanced ratios between source and target domains. For example, in the office dataset the ratios range between 1.87 to 6.59;[42] for the extended office-Home dataset the ratios are close to 1;[43] and for the Photo-Art-Cartoon-Sketch (PACS) dataset the ratios range from 1.14 to 2.35.[44] In the presented dataset, the Smart Maintenance Living Lab (SMLL), the ratio ranges from 8.6 to 21.6. This means that less data is available for each target domain. Finally, (iii) there is considerable heterogeneity in the source domain which makes non-TL tasks already hard to generalize, as it has been extensively reported in similar datasets such as Pronostia,[45] IMS[46] as well as

SMLL.[47] Although this last issue can also be the case in image classification tasks, there is no clear way of comparing degrees of heterogeneity for this purpose.

So far, the works of TL applied to the domain of PdM have been limited, and when available have focused on the supervised fault classification task. Other areas, such as RUL (supervised regression) and AD (unsupervised), which are inherently more challenging, have received limited attention in TL research. The authors consider that this may be due to the limited amount of large datasets for training reliable baseline models, and the challenge posed in detecting anomalies or predicting RUL in datasets that are inherently dissimilar.

2.3. Lightweight models and MobileNet

Since the middle of the 2010's, and together with the advent of successful deep learning models, the case has been made in favor of so called lightweight deep learning. Although there is no formal definition for what qualifies as a lightweight model, it is most often presented as optimizations with respect to well-known large deep learning models. The growing interest towards lighter models comes from the fact that a lower number of parameters reduces training and inference time, furthermore, it has also been demonstrated that smaller models can increase performance and generalization. For example, when LeNet-5 was first introduced in 1995 it consisted of 1 million parameters and was the cornerstone in character recognition.[48] Progress over the next years would be mainly achieved by increasing the network size, in 2014 VGG-16 was introduced,[49] it consisted of 138 million parameters and was at its time the best performing model for the ImageNet dataset; the model was quickly outperformed by others such as ResNet in 2015 with with 60 million;[34] and SimpleNet in 2016 with only 6.4 million parameters.[50] This highlights the trend of reducing the number of parameters by improving the architecture rather than increasing the number of parameters.

The concept of lightweight has been addressed in regards to different aspects such as reducing the number of parameters of well-known models by pruning the weights;[51,52] compressing the model weights by using hashing functions;[43] reducing the numerical precision of the learned weights;[53] among other techniques.[54] However, most of these approaches focus in reducing inference time after having trained a large network. In contrast, other approaches have focused in creating architectures which are also easy to train, such as SqueezeNet,[55] Simplenet,[50] NASNet[56] and the Mobile Networks (MobileNet).[57] This work focuses on the usage of MobileNets and although other architectures could be considered for the same methodology presented here. MobileNets are a family of architectures aimed at enabling computer vision applications for mobile devices. In order to achieve this, the architectures use a considerable lower number of parameters, and replace the standard convolutional operator with a depth-wise separable convolution. Separable convolutions are notorious for enabling a reduced number of multiplications while still performing in pair with state of the art models for object detection.

The use of lightweight models in PdM is relevant to today's industrial applications as it allows monitoring of equipment on edge devices and without the need of GPUs. Recent research has proven its advantage over large deep learning models in PdM tasks, for example, a MobileNet V2 architecture was extended to include a channel attention mechanism and proved successful in the fault bearing diagnosis of the CWRU dataset.[58] Their results proved to be more accurate

(80.60%) and faster in comparison with deep architectures such as AlexNet and Res-Net-50 with accuracies of 58.6% and 78.78% respectively. In addition to this, the model reduction is smaller in memory and has faster inference times. Other publications have achieved even higher performance on the CWRU dataset using an earlier version of the network, namely the MobileNet V1, with an accuracy of 96%.[59] Some approaches have also considered lightweight models in combination with weight pruning, for example, the MobileNet V2 with weight pruning was evaluated for bearing fault diagnosis under different degrees of sparsity. Their study found a minimal decrease in the model's accuracy despite considerably pruning, in fact, a moderate amount of pruning proved to give the best results.[60] Their results compare the diagnosis using LeNet-5, 98.74%, against the original MobileNet V2, 99.58%, and MobileNet V2 with a sparsity of 0.3, 98.95%. The dataset used is collected by themselves, therefore the results cannot be compared to other benchmarks. These results show that lightmodels are well suited for PdM tasks, provide considerable benefits for real applications that require low computation, and in some cases provide better results than standard models.

To the best of our knowledge, transfer learning using MobileNets has only been used in the context of image recognition tasks. For example, for evaluation of asphalt quality,[61] or steel frames' damage.[62] The pre-trained MobileNet uses the real ImageNet dataset, and as discussed in Section 2.2, these weights should not be expected to provide any information for downstream tasks that use representations such as spectrogram. Due to this, the authors considered that there is limited work on using MobileNet for spectrogram analysis.

Finally, Table 1 provides a comparison of the number of parameters and computational complexity for popular image recognition models. Figure (1) shows a visual comparison of different models' performance in the ImageNet classification task. Notice that the selected architecture for this paper, namely the MobileNet v2, is an extremely fast and compact model, and it formas part of the Pareto front for optimal model selection. For a broader array of more recent image recognition models, a comprehensive survey can be found in the work by Bianco et al.,[63] although it mainly includes models with even higher complexity. Importantly, it must be emphasized that these comparisons serve as reference points and may not directly indicate the most suitable model choice for either anomaly detection or transfer learning.

3. SMART MAINTENANCE LAB DATASET

The Smart Maintenance Living Lab (SMLL) is an open test research platform that aims to support the adoption of condition monitoring technologies.[1] The platform consists of a fleet of seven identical drive-train setups that perform accelerated lifetime tests on FAG 6205 bearings. The fleet offers two advantages: first, it allows faster data collection; and second, since identical drive-train systems can have variability, it offers the opportunity for training and evaluating robust models.[1,66] The data is rich in the variety of operating conditions such as speed and loads, in addition to speed changes while operating. This is a considerable improvement against most available benchmarks, which tend to be limited to a dozen or less tests, and in most cases, have a limited number of operating conditions.

Table 1: Model comparison across popular deep learning architectures. Parameters and Multiply-Add Accumulate (MACC) are reported based on the respective benchmarks while inferring for the ImageNet dataset. For the model presented here no estimation of the MACC is provided as it is not intended to be used with ImageNet and input size is a crucial parameter for determining the number of parameters and required computations.

Network	**Year**	**Parameters**	**MACC**
AlexNet[50]	2012	60.97 M	7.27 G
VGG16[50]	2014	138.36 M	154.7 G
ResNet-152[50]	2015	60.19 M	11.3 G
SimpleNet[50]	2016	6.4 M	1.9 G
SqueezeNet[50]	2016	1.25 M	861 M
NASNet-A (4@1056)[56]	2017	5.3 M	564 M
NASNet-A (3@960)[56]	2017	4.9 M	558 M
MobileNet V2 1.0[64]	2018	3.4 M	300 M
MobileNet V2 0.35[64]	2018	1.6 M	59.2 M
MobileNet V3 Large 1.0[64]	2019	5.4 M	219 M
MobileNet V3 Large 0.75[64]	2019	4.0 M	155 M
MobileNet V3 Small 1.0[64]	2019	2.5 M	56 M
MobileNet V3 Small 0.75[64]	2019	2 M	44 M
Mini MobileNet V2 (ours)	-	26 K	NA

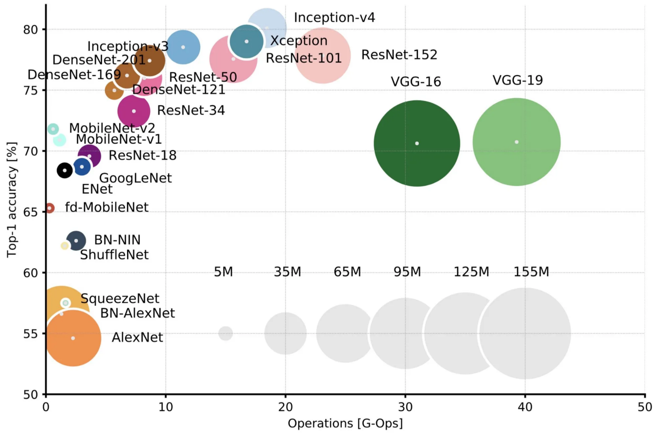

Figure 1: Top-1 accuracy vs. operations (inference) and network size for selected architectures. The size of the blobs is proportional to the number of network parameters. Figure by Canziani et al.[65]

As of the time of writing, the SMLL dataset [1] consists of 145 bearing tests, however, data collection is ongoing.

3.1. Data Collection

Tests are performed under different speeds, loads and initial conditions. These variations are meant to represent different possible operating conditions. The speed of a test can either be constant or follow a saw-tooth profile. Constant speeds are set to a fixed value between 1500 rpm and 2100 rpm. In the saw-tooth profiles the speed varies from 1000 rpm up to 2000 rpm. The test starts at a speed of 1000 rpm and is increased in steps of 100 rpm. Each speed is kept constant for 60 s, and once the speed reaches 2000 rpm the speed is set back to 1000 rpm. The saw-tooth profile tests were captured to obtain more variability in the data for each test. The load of the tests is fixed to a value between 8 kN and 9 kN.

[1] Dataset is available upon request at Flanders Make website https://www.flandersmake.be/en/datasets

Finally, the initial condition indicates whether the bearing is indented at the start of the test. The indentations of the bearings are meant to accelerate degradation. The indentations are done in the inner race using a Rockwell C hardness tester, and have diameters are within 400 ± 25 μm. These indents are small such that the bearing can be considered healthy at the beginning of the test but significant enough to guarantee that the degradation onset occurs within some hours. Notice that the assumption here is that indented bearings behave as healthy bearings at the beginning of the test, however it is important to mention that already clear differences exist in the spectrogram content. Despite this, there is a considerable long steady state in which vibration profile does not change, which indicates that no further degradation is occurring on the bearing. The outcomes of each test are also reported, which can be either that the bearing remains healthy or damage is detected. Each report contains information concerning the condition of the bearing components, in addition to a report of events during the tests, and photos of the end condition of the rolling elements, rings and axles of the setup.

Tests are measured with vibration sensors. The vibration signal is sampled at 50 KHz. In early tests, a sample was collected every 10 s, while for later tests the samples were collected every second. Most of the tests correspond to the second case.

The stop condition differs, depending on whether the bearing is indented or not. In the case of unindented bearings, this is defined as the moment when the temperature stabilizes and at least a period of two hours has passed. In general, unindented bearings are not expected to fail as their expected lifetime exceeds the testing period. During evaluation of these bearings, no anomalies were reported and during examination of their conditions no damage was found. For the indented bearings, the stop condition is the moment that the peak vibrations reach a magnitude of 20 g. For a small number of bearings, this condition is not reached and tests are stopped after a few hours. These bearings do undergo degradation and anomalies are reported, but due to safety reasons the tests had to be prematurely stopped.

Figure (2) shows examples of damaged bearings after the accelerated life tests.

3.2. Source and Target Datasets

This research focuses on anomaly detection under the transferal between different operating conditions. The scenario involves training an anomaly detection algorithm to perform well at a specific speed and exploring its performance under a different speed with limited sample availability. In this research, the evaluation focuses solely on tests conducted with a load of 9 kN, as it is the load with more speed-varying data available. The source domain corresponds to the configurations with a load of 9 kN and speeds of 1000 and 2000 rpm, which correspond to the minimum and maximum operational speeds. The source dataset contains both indented and non-indented bearings. The target dataset corresponds to tests with a load of 9 kN and speeds between 1000 and 2000 rpm, so that the transfer learning step corresponds to a speed interpolation. Table 2 summarizes the amount of recorded hours for each speed.

The source dataset consists of 72 bearing recordings, of which 64 are tests performed with a load of 9 kN and 2000 rpm, and 8 are tests performed with the saw-tooth speed pattern. From this data, 13 bearings are used as validation data for

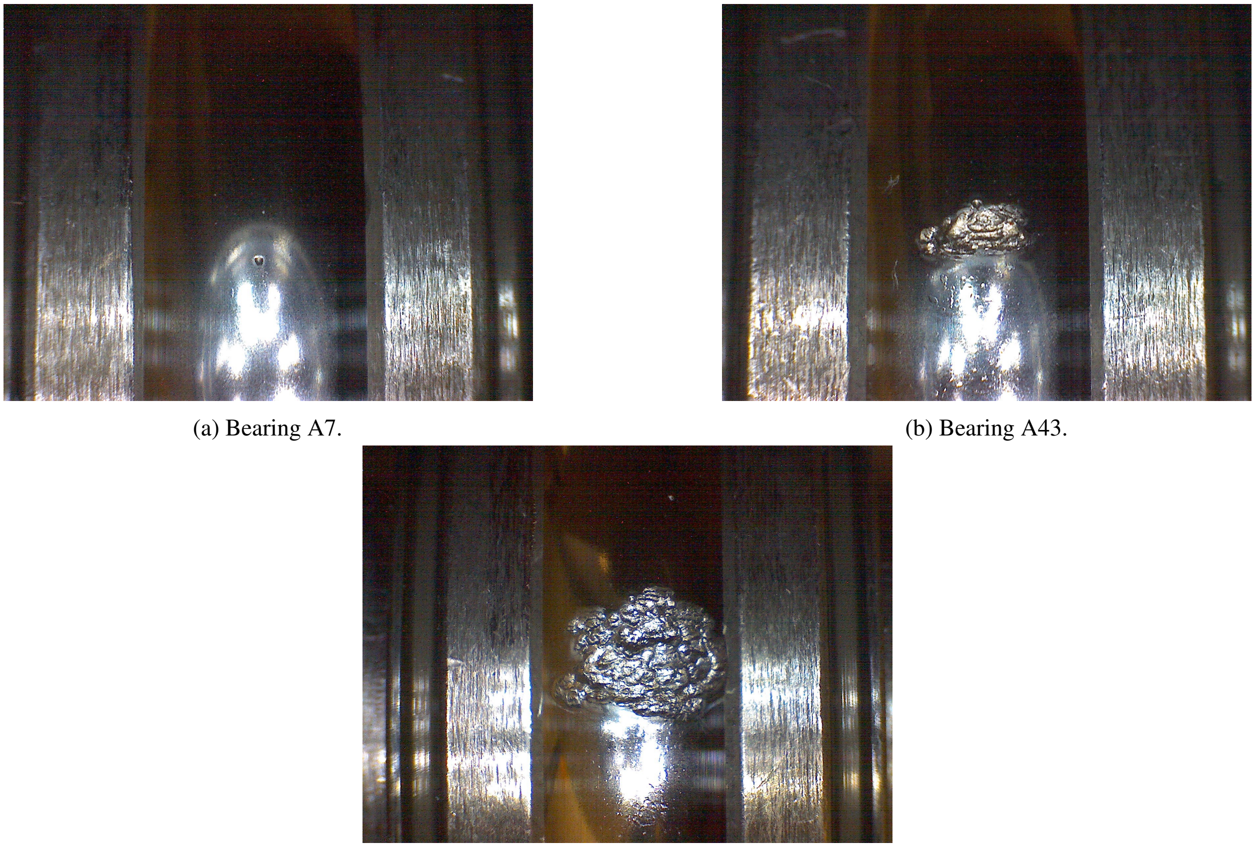

(a) Bearing A7.

(b) Bearing A43.

(c) Bearing A47.

Figure 2: Details of the bearings' condition before and after testing. Top) Bearing A7 with a small indentation to induce accelerated degradation. The indentation is located at the inner race and has a diameter of approximately $400 \pm 25\ \mu m$. Middle) Bearing A43 with a moderate amount of damage after the test. Bottom) Bearing A47 with extensive damage after the test. For reference, the inner race diameter of the FAG 6205 is 25 mm.

Table 2: Sample size in hours of recording for each speed.

Speed	Train	Evaluation	Domain
1000	2.3 h	4.2 h	Source
1100	2.5 h	4.6 h	Target
1200	2.6 h	4.6 h	Target
1300	2.5 h	4.7 h	Target
1400	2.5 h	4.7 h	Target
1500	2.5 h	4.6 h	Target
1600	2.5 h	4.6 h	Target
1700	2.4 h	4.6 h	Target
1800	2.4 h	4.6 h	Target
1900	2.4 h	4.6 h	Target
2000	48.3 h	154.2 h	Source

parameter tuning and prevention of overfitting. From the saw-tooth speed profile recordings, only the segments at the lowest speed (1000 rpm) are used as part of the source dataset.

The target dataset consists of 14 bearing recordings, all of them with saw-tooth speed profile. From these, 8 correspond to the same bearings in the source dataset but for the segments where the speed is different than 1000 or 2000 rpm. In addition, 6 completely separated tests are included. Table 3 summarizes the source and target datasets.

Table 3: Summary of the dataset and experiment conditions.

	Dataset	
	Source	Target
Bearing type	FAG 6205-C-TVH	
Initial condition	- Healthy - Indented (400 ± 25 μm)	
Stop condition	- Healthy: 2 hrs after stable temperature - Indented: Vibrations exceeding 20 g or after several hours without failure.	
Sampling rate	50 kHz	
Acquisition frequency	- Every second - Every 10 seconds	
Speed pattern	- Fixed - Sawtooth	- Sawtooth
Operating speeds (rpm)	1000, 2000	1100, 1200, 1300 1400, 1500, 1600 1700, 1800, 1900
Operating load	2 kN	
Number of tests	- Fixed speed: 64 - Sawtooth profile: 8	- Fixed speed: 0 - Sawtooth profile: 14

4. METHODOLOGY

4.1. Spectrograms and Mel Spectrograms

The vibration signals are transformed into spectrograms using the short-time Fourier transform (STFT), and using log transformation to obtain the mel spectrogram. A spectrogram is a representation of the frequency content over time for a given signal, whereas the mel spectrogram is a transformation that applies a logarithmic scale to the high frequencies while preserving a linear scale for the lower frequencies. The mel spectrogram representation reduces the number of frequency components to a defined number of mel-frequencies. After initial tests, the mel spectrogram representation was preferred due to its compressed frequency dimension as most of the faults are found within the low frequency band. In general, reducing the number of input features allows for deep learning models to require less parameters. Figure (3) shows an example of the signal in time and the two frequency representations. Finally, the log mel energy of the spectrogram is calculated and used as the features. Notice that in the mel spectrogram representation, the higher contrast between adjacent frequencies is due to the logarithmic scaling.

4.2. Anomaly Detection

The goal of this research is to train models that are able to detect anomalies, specifically the first anomaly during a test, which often corresponds to the degradation onset. This can be beneficial for predictive maintenance tasks, such as better Remaining Useful Life (RUL) estimations as well as optimizing maintenance schedules. The AD task needs to

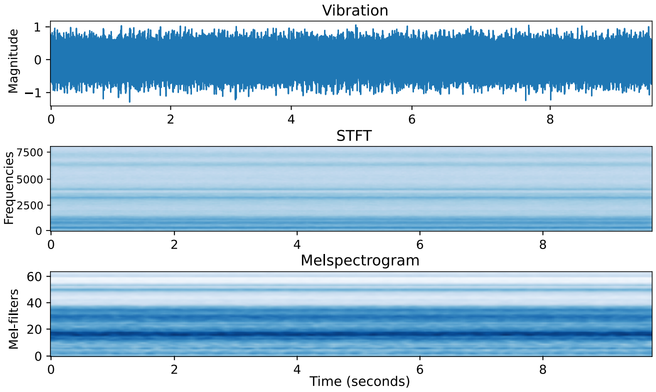

Figure 3: Vibration signal in time and its representations as spectrogram and mel spectrogram.

be unsupervised, meaning no labeling should be assumed. In order to accomplish the task, the models are trained to predict the operating speed over healthy data; or in the case of indented bearings, the beginning of the test which can be considered as healthy. When bearings start to degrade, the models will predict erroneous speeds as this is unseen data. The difference between the predicted speed value and the actual speed can be seen as a health indicator that can be used for AD. This approach is similar to the more commonly used auto-encoder (AE) method in which the original signal is compressed and afterwards reconstructed. In the AE case, unseen inputs propagate as data points distant from the embedding centroids, which in turn causes large reconstruction errors. In an analogous way, the difference between the predicted speed and the actual one is used instead. To be clear, although data labels are used to train the network, the task of anomaly detection remains unsupervised as no information about these events is provided during training.

The target of the neural network corresponds to the min-max normalized speed value. In the baseline model, this corresponds to either 0.5 for 1000 rpm or 1 for 2000 rpm. For the target domain, the speeds are in-between 0.5 and 1.

To detect anomalies, an error threshold needs to be defined. In supervised AD, this is achieved by optimizing a threshold value using the labeled example, for example, thresholds can be defined based on a percentile of the reconstruction error over several complete tests, e.g., 95% of the upper value, or based on visual examination of the temporal trends of the reconstruction error. Other options for the supervised scenario can use asymmetric cost functions that enforce greater important to the correct classification of anomalies. Due to the nature of this research, supervised approaches to determine the threshold cannot be used and instead the threshold is defined in an online approach. For each test, the threshold is defined based on the reconstruction error over the training period, or the first 25 minutes for hold out test bearings. The threshold is defined as the sum of the 95th percentile (P_{95}) plus the 10th percentile (P_{10}). The P_{95} value was selected to avoid outliers which may occur during the startup period of the test.

4.3. MobileNet V2

All models presented follow the MobileNetV2 (MNv2) architecture.[67] This architecture uses depth-wise separable convolutions and connected residuals over the bottlenecks which allow inducing meaningful representations. The key component of MNv2 is the bottleneck unit presented in Fig. (4). Each bottleneck unit consists of three sub-units: an expansion layer that extracts features from the input expanding the input to a given number of filters defined by the expansion parameter; a depth-wise convolution layer that convolves each of the expanded outputs separately; and a projection layer that reduces redundant information. This architecture is selected due to its fast training and successful use in image classification tasks.

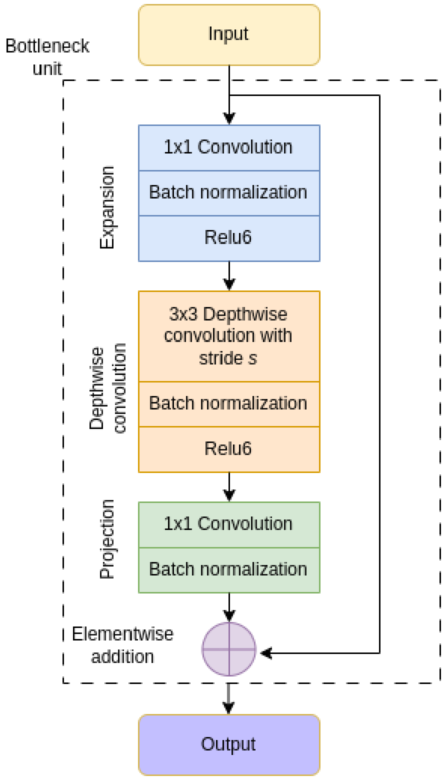

Figure 4: Bottleneck units of the MNv2 are composed of three stages, namely an expansion, a separable convolution and a compression stage (projection and element-wise addition).

The original MNv2 model is trained to recognize real life images.[67] However, the problem at hand uses spectrograms as input images to the network and instead the weights were initialized at random. In some cases, MNv2 or similar architectures are reused using the weights learned from training on imagenet.[16] This is an important difference as we consider that the patterns generated by the convolutional filters are likely to differ between real life images and spectrograms. Finally, the original MobileNetV2 consists of approximately 3,400,000 parameters, with differences depending on the selected width parameter. The considerable amount of parameters allows MobileNetV2 to learn a broad range of images, however, the dataset at hand is considerably smaller than image recognition datasets. To improve training time and generalization performance, a smaller version of the MobileNetV2 architecture is used; this consists of a lower number of layers and less convolutional kernels. The proposed architecture consists of approximately 26,000 parameters. Table 4 describes the architecture, where each bottleneck corresponds to a 3 layer unit as described in Fig. (4). Notice that the column *n* corresponds to the number of units, which in this case is kept constant to 1, whereas the original MobileNetV2 uses multiple blocks consecutively.

Table 4: Reduced MNv2 architecture. Where *c* corresponds to the number of channels, *n* the number of times the given layer is repeated, and *s* the stride.

Operator	*c*	*n*	*s*
Conv2D (3x3)	16	1	2
Bottleneck	32	1	1
Bottleneck	64	1	1
Bottleneck	64	1	1
Conv2D (3x3)	128	1	1
Global Avg. Pooling	-	1	-
Dense	-	1	-

4.4. Baseline Model

The baseline model is an MNv2 model trained to achieve high efficiency in the source domain, specifically the tests performed at 1000 and 2000 rpm. For each test, only the first 35% of the samples are used for training or validation, with a maximum of 2000 samples. This segmentation is based on the assumption that during this period, indented bearings can be considered as healthy. The same assumption also applies to unindented bearings, although considering the slow degradation process, it would be reasonable to assume an even longer period. However, this is not considered in the current work. Based on this segmentation, the remaining samples in a run are used as test data, with a limited degree of information leakage due to serial correlation.

The optimizer used is Stochastic Gradient Descent (SGD) with learning decay and early stop to prevent overfitting. The optimizer's parameters and data input representation are selected using grid search over the ranges shown in Tables 5 and 6, respectively. The selection is based on repeated 5-fold hold-out validation. The best parameters are found to be a batch size of 128, a learning rate of 0.001, a temporal width of 49, and 64 mel frequencies. It is worth noting that the differences in data representation (Table 6) and the batch size had a negligible effect.

Table 5: Grid search parameters.

	Parameter	Range
Optimizer parameter	Batch size	64, 128, 256
	Learning rate	0.01, 0.005, 0.001

Table 6: Data representation parameters.

	Parameter	Range
Data parameter	Temporal width (data points)	49, 98
	Spectral width (Mel frequencies)	64, 128, 256

4.5. Transfer Learning by Fine-tuning

The fine-tuned model uses the embedding layer after the global average pooling of the baseline model (see Table 4), followed by a dense layer of 64 units with ReLU activation. The baseline model is finetuned using the target domain

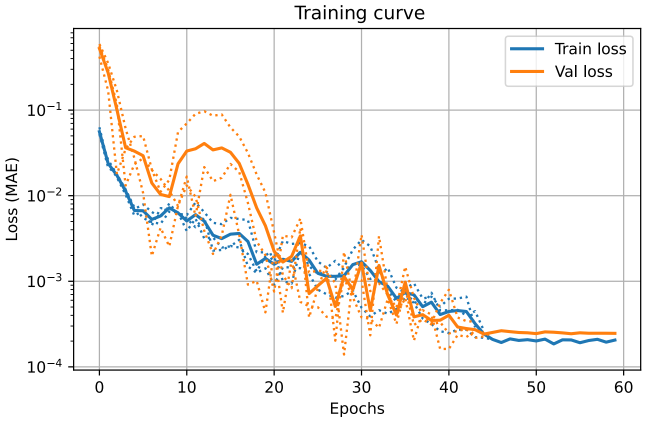

Figure 5: The 5-Fold validation curve for the best parameters found.

data, therefore obtaining an adapted model for each new target speed. The models are trained using back propagation with the same parameters as the baseline model. For this purpose, 11 of the bearings are used for training and 3 for validation, following a split of 78% for training and 22% for validation. Similar to the training of the baseline model, only the first 35% of a run samples (up to a maximum of 2000 samples) are used for training, while evaluation is carried over the rest of the run. The fine-tuning uses the best hyperparameters found while tuning the baseline model, employing SGD as optimizer with learning decay and early stop.

5. RESULTS

This section presents the results for the baseline model and the transfer learning. The task at hand is to detect the first occurrence of an anomaly, typically associated with the onset of degradation. However, the tests are run until a stop condition is reached, and there is no way of determining when this actually occurs. A subset of bearing tests was manually inspected, and experts labeled the time at which degradation starts based on the vibration magnitude. There are 9 bearings with available timestamps. In addition to this, a final report is available for each bearing where the final conditions and type of failure are specified.

The first evaluation concerns the time difference between the predicted first anomaly and the reported label. In general, it is a good sign if the model detects anomalies before the time labeled by the experts as this would point towards above expert knowledge capabilities. However, this can easily be obtained by simply reporting anomalies since the beginning of the test, which would be evident false positives. For the current experiments, there is no exact way of determining this time limit, therefore these values need to be assessed with some reservations. Equation (1) shows the formula for the percentage difference ($perc_{error}$), given the anomaly detection time (t_d), the expert's reference (t_r) and the total length of the experiment (T_t). Here, positive values correspond to detections ahead of time and negative values correspond to delayed detections.

$$perc_{error} = 100x(t_d - t_r)/T_t \tag{1}$$

The second evaluation concerns the state at the end of the test, which can be either damaged or healthy, and is based on the end test report. For this evaluation the accuracy, precision, and recall are reported. The formulas for accuracy, precision and recall are shown in Eqs. (2), (3), and (4) respectively. In these cases the true positives are anomalies correctly detected, and the abbreviations are as follows: true positives (TP), true negatives (TN), false positives (FP) and false negatives (FN).

$$Accuracy = \frac{TP+TN}{TP+TN+FP+FN} \tag{2}$$

$$Precision = \frac{TP}{TP+FP} \tag{3}$$

$$Recall = \frac{TP}{TP+FN} \tag{4}$$

5.1. Baseline Model Performance

Table 7 presents the results for the first anomaly detected against the expert's reference. For the two bearings with available labels, bearings A83 and A84, the anomalies are detected with a delay of 50 s and ahead by 4870 s (81 min) respectively. Figures (6) and (7) show the results for bearing A83, and Figs. (8) and (9) for bearing A84. The labeled anomaly corresponds to the sudden increase in the prediction error. The detection threshold was not tuned as this would require observing the error rates of the bearings after the training phase, which would defeat the purpose of making a fast-transferable approach. Notice that the missing data points for bearing A84 correspond to periods in which the machine was stopped.

Table 7: Baseline results, showing the difference between the anomaly detection and the reference timestamp.

Bearing	Total duration (s)	Reference (s)	First detection (s)	Diff.	% Diff.	Abs % diff.
A83	7 930	7 100	7 090	10	0.14	0.14
A84	35 538	33 478	28 608	4 870	14.55	14.55

The results of the evaluation of the final bearing condition are summarized in Table 8. The obtained accuracy is 98%, with only one one out of eighteen healthy bearings being classified as anomalous, namely a precision of (P=94.4%); a perfect recall (R=1); and no false negatives (FN=0). Figure (10) shows the target and predictions for an unindented bearing which does not fail during the test. Figure (11) shows the predictions against the selected threshold, at no moment the prediction error surpasses the threshold. In summary this shows that the baseline model has a great sensibility for detecting anomalies and that in no instance it causes false positives.

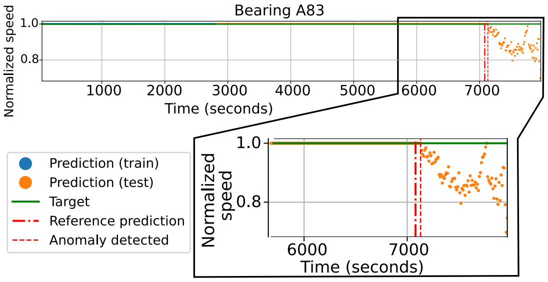

Figure 6: Normalized speed predictions for indented bearing A83. The anomaly is correctly detected in the proximity of the reference timestamp.

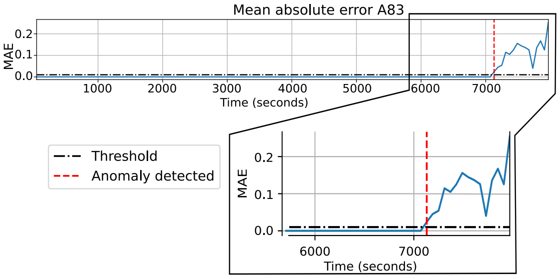

Figure 7: Mean error and first reported anomaly for indented bearing A83. The anomaly is reported the moment that the prediction error surpasses the threshold.

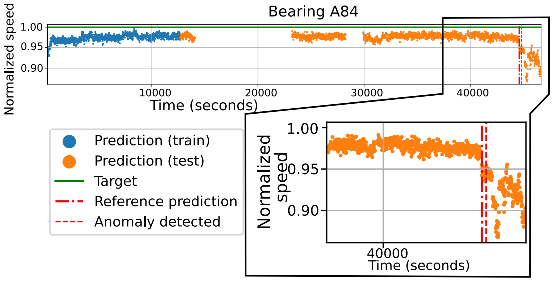

Figure 8: Normalized speed predictions for indented bearing A84. The anomaly is correctly detected in the proximity of the reference timestamp.

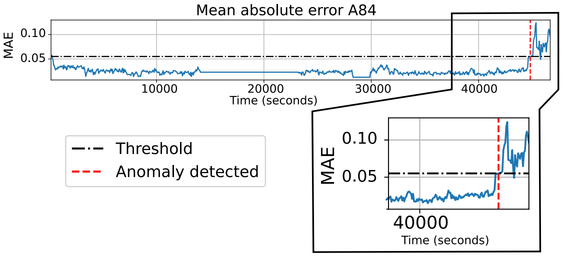

Figure 9: Mean error and first reported anomaly for indented bearing A84. The anomaly is reported the moment that the prediction error surpasses the threshold.

Table 8: Confusion matrix of the baseline model.

		Predicted	
		Anomaly	Healthy
Actual	Anomaly	100%	0%
	Healthy	2.22%	97.77%

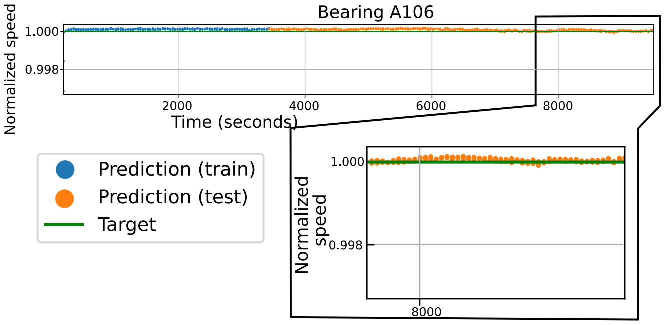

Figure 10: Normalized speed predictions for unindented bearing A106.

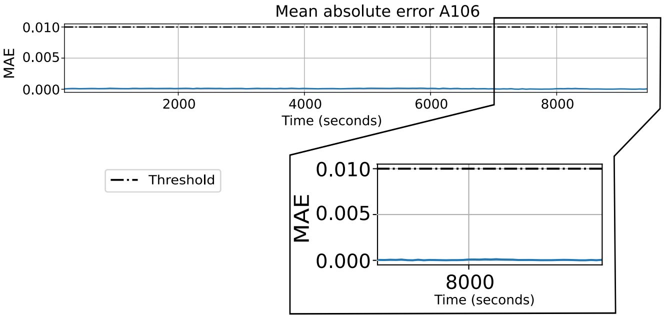

Figure 11: Mean error for unindented bearing A106. The threshold is not surpassed, hence no anomaly is reported.

5.2. Transfer Learning Performance

After demonstrating the effectiveness of the baseline model in identifying vibration patterns to diagnose the bearing condition, the TL by fine tuning is evaluated. Table 9 presents the results after training for the validation data, which corresponds to the beginning of the test for 3 hold-out bearings. The results provide an indication of how well is the model adapted to the target data over previously unseen data. The TL advantage is clear as the error estimation is one order of magnitude smaller than the baseline reference. Interestingly, the errors obtained for the model that only uses the target data are larger than the baseline, which points to an underfit scenario, most likely due to insufficient training data. The expected result is that the baseline model will be more likely to predict false positives, whereas the model trained with only the target data will be unable to detect anomalies.

Table 9: Validation results (mean absolute error) for each model over all the folds for the validation data.

Target speed	Baseline	Only Target	Transfer learning
1100	0.188 ± 0.016	0.179 ± 0.196	0.028 ± 0.015
1200	0.137 ± 0.076	0.485 ± 0.066	0.013 ± 0.003
1300	0.208 ± 0.069	0.439 ± 0.199	0.013 ± 0.002
1400	0.071 ± 0.015	0.451 ± 0.214	0.019 ± 0.005
1500	0.096 ± 0.019	0.498 ± 0.156	0.019 ± 0.008
1600	0.190 ± 0.100	0.706 ± 0.014	0.021 ± 0.005
1700	0.129 ± 0.080	0.636 ± 0.097	0.021 ± 0.005
1800	0.222 ± 0.190	0.706 ± 0.126	0.015 ± 0.004
1900	0.245 ± 0.081	0.886 ± 0.110	0.015 ± 0.006
Mean	0.165	0.554	0.018

The transfer learning models are able to detect anomalies ahead of time or with a small delay with respect to the reference value. Table 10 summarizes the results and compares them against the baseline, which is the model without fine tuning. The results from the baseline trained using only the target data are not presented as these models failed to detect the anomaly in all cases. Notably, the baseline model tends to predict anomalies considerably ahead of the reference, attributed to large prediction errors due to the new operating condition being unseen during the training of the model. Whether this is a false positive or a better performance is difficult to assess as bearings are only visually inspected at the end of the test. The models trained using only the training target data underfit and fail to detect anomalies due to the insufficient amount target speed data.

Table 10: Results for transfer learning. The reference corresponds to the annotations made by experts. Positive differences correspond to detections ahead of the reference whereas negative differences correspond to delayed detections.

			Baseline			Transfer learning		
Bearing	Total duration	Reference	First detection	Difference	Abs Pct Diff	First detection	Difference	Abs Pct Diff
A146	28261	28031	11540	16491	58.35	15120	12911	45.68
A148	8670	6760	7400	-640	7.38	7100	-340	3.92
A150	12370	10150	6000	4150	33.55	4630	5520	44.62
A151	18320	18280	8940	9340	50.98	11890	6390	34.88
A154	7680	5940	4620	1320	17.19	5990	-50	0.65
A155	23051	20681	8580	12101	52.50	20951	-270	1.17
A156	44412	42162	25741	16421	36.97	28251	13911	31.32
A158	19821	19821	7260	12561	63.37	10630	9191	46.37
Mean					38.19			26.08

With respect to the end result, both the baseline model and the adapted model are able to detect anomalies in all 14 indented bearings before the end of the test (This corresponds to an accuracy of 100% and a precision of 100%. Note, however, that TN and FN are note defined as no healthy bearings are evaluated in the transferred models). This indicates the robustness and effectiveness of the models in identifying anomalies. However, the validation results presented in Table 9 demonstrate the superiority of the TL approach. TL models have smaller validation errors for the target conditions, and their predictions are closer to the expert's reference. In summary, the TL models outperform both the baseline and target-only models. This highlights the value of leveraging the knowledge learned from the abundant source domain to improve the anomaly detection performance in the target domains.

5.3. Discussion

The presented research focused on the accurate detection of anomalies in online settings. Although straight-forward evaluation of AD is difficult due to the nature of the experiments, a number of degradation onsets were defined after visual examination of the vibration signal, in addition to inspection of the bearing status at the end of the test. The interest in identifying anomalies lies in its potential use for monitoring conditions, as well as an agnostic approach for early fault detection. Furthermore, the correct identification of the first anomaly is a useful indicator for constructing health indicators and remaining useful life estimation.[47] Overall, we argue that correctly detecting anomalies can bring value to monitoring technologies and offers advantages over requirements posed by supervised learning techniques.

The focus of this research lies in achieving precise anomaly detection within online scenarios. The evaluation of anomaly detection (AD) is inherently intricate due to the experimental nature; nevertheless, numerous degradation onsets were established through visual scrutiny of vibration signals, coupled with assessment of bearing status upon test conclusion. The impetus behind anomaly identification stems from its potential utility in condition monitoring, as well as its unbiased application in early fault detection. Additionally, accurate pinpointing of the initial anomaly serves as a valuable indicator for constructing health metrics and estimating remaining useful life.[47] In summary, we contend that the accurate detection of anomalies adds value to monitoring technologies and holds an advantage over the prerequisites posed by supervised learning techniques.

In contrast to many other studies in the field where models are evaluated based on their ability to accurately classify faulty and healthy samples, this research approached the challenge of online anomaly detection by precisely determining the time of occurrence of the first anomaly. Therefore rather than focusing on accuracy or precision, the performance was focused in the time delay or overhead of detecting a single anomaly per bearing. This emphasis was chosen due to the critical nature of detecting the initial anomaly in numerous real-world applications, as it often signifies machinery failure or, in the context of bearings, marks the onset of degradation. Extra anomalies detected afterwards can also be informative but they may be trivial to detect, or be reported too late to be useful for decision making. In addition to this, a practical consideration when deploying monitoring solutions is the reactive actions that need to be taken. In order to obtain more robust results one could also consider training models to optimize the precision or recall of the models based on a cost of decision making, where the false positive and false negatives incur specific costs and the end goal is to reduce their respective risks. For example, as shown in Table 10, the baseline models are incurring considerable false positives, while the transferred models incur in three cases false negatives which are shortly after detected (less than 6 minutes). Expert knowledge can be used in these cases to select the most convenient trade-off between both metrics.

The transferal challenge investigated concerns scenarios where the is limited data in the target domain. The presented TL model uses a small fraction of data, which in combination with a small architecture allows training a model within minutes, which means the models can be effectively adapted and deployed to monitor a new bearing. Notice that only the first 35% samples are used, and this under an extreme imbalanced transferal scenario. Due to limitations in the number of available labeled bearings, data from within a run was used to train the baseline and the transferal models. As previously mentioned, this can lead to a small degree of information leakage due to samples from the training and validation being temporally correlated with the test data. Further reducing the train margin (bellow the 35%) could make the evaluation more rigorous. Notice that results were also presented for a set of hold-out tests in order to demonstrate that the generalization is valid over unseen bearings, where no information leakage occurs. As more data becomes available, a more detailed evaluation can be done in order to measure correct generalization, or alternatively a more rigorous evaluation by means of repeated cross-validation. Overall, this shows how the presented methodology can be trained and adapted easily in real settings, as it would only require a few minutes of incoming data to be adapted to previously unseen conditions.

An important caveat to address concerns the model selection approach. As explained in Section 4.4, the best model is selected based on the mean absolute error of predicting the operational speed. This optimization procedure does not necessarily corresponds to finding the best model for anomaly detection. Neither does it imply the reported error rate is more reliable. In fact, the reported error is not a parameterized value, and cannot be compared across models. In other words, we can only rely on the changes in the prediction error, but the magnitudes reported by different models are not comparable as these are not distance metrics. In addition to this, research has empirically shown that models trained to perform better on a given task may lead to underperforming transferable models.[68] At this point, this is still an open question which is still been researched in the field and that should be considered in future research.

Finally, the presented work used the minimum and maximum speeds for the baseline models, however, other speed combinations are possible. The current example demonstrates a case of interpolation, where the new speeds are within the seen data. Extrapolation scenarios, where the speeds are outside of the range, can also be addressed following this methodology. However, notice in Table 2, that the sample size for tests with a speed different than 2000 rpm is considerably smaller.

6. FUTURE WORK

After this research some future research tracks are proposed as follows:

1. Basis function decompositions. One of the crucial steps in PdM tasks is the preferred data representations. This research chose the mel spectrogram due to its compact representation. However, other spectral representations could be considered and evaluated. For example, wavelet and chirplet transforms can generate multi-resolution representations in frequency and time, which could benefit from richer features and allow anomaly detection at a more fine-grained time resolution. Furthermore, different families of basis functions can provide enhancement to the expected patterns. In this particular case, the vibration patterns of healthy bearings can be described by wavelets such as Daubechies and Morlet, which can be enhanced using these type of basis functions. Furthermore, recent works have shown ways of learning basis functions and their parameters via deep learning[69] in the context of condition monitoring.
2. Data augmentation. Early work in this research used data augmentation techniques from SpecAugment,[70] frequency masking and time masking, with the goal of improving the validation error of the baseline model. This proved to be effective, however, the obtained robustness was such that the model was able to correctly identify the operational speed even if the signal was considerably distorted due to degradation. Data augmentation has proven to be extremely useful in assisting training deep learning models and should be also considered in the context of transfer learning. Some methods that should be considered include data transformations,[6] and generative approaches.[71] Furthermore, modifying the objective function of the presented baseline model could

allow the SpecAugment to be used, for example, by finding structures using self-supervised learning instead of supervised learning.

3. Transfer learning for specific scenarios. In recent years the field of transfer learning has gained much attention in more specialized methods. This work presented a classical fine-tuning approach, which has become a common standard due to is ease of deployment, however, it is only suited for supervised scenarios in which a sufficient amount of labeled data exists. More recent approaches that could be investigated and are relevant for industrial applications include: adversarial learning for self-supervised or unsupervised transfer;[72] few-shot learning for anomaly detection for scenarios where few labels are available in the target domain;[73] as well as the integration of explainability for TL-AD.[74]

4. Advanced architectures. Finally, more recent lightweight architectures such as MobileNetV3[64] and EfficientNet[75] could be considered. Although as discussed in this research, efficiency in a pre-trained task does not guarantee best results for a transfer learning.

7. CONCLUSION

This study presents the successful implementation of a transfer learning approach to adapt a neural network for bearing diagnosis under new operating conditions. The transferability is evaluated on a selected number of runs whose vibration signals were carefully inspected, in addition to the bearings' outcomes after the tests were conducted. The objective is the identification of anomalies in an unsupervised way, meaning, no labels are provided for these events.

The results show that the baseline model trained only on the source data has a high accuracy for anomaly detection in the source domain (accuracy 98% and precision 94.4%), and that the adapted models derived from it are able to learn the new operating conditions with a limited amount of samples. It was found that the baseline model trained with the source domain and the adapted model were able to detect all the anomalies in the target domain (accuracy 100% and precision 100%). Whereas the model trained using the target domain data had insufficient information and underfitted, causing it to be unable to detect any of the anomalies (0% accuracy).

When comparing the detection precision it was found that the adapted models provided predictions more in line with the expert's knowledge. An absolute percentage difference of 26.08% was obtained for the adapted models, and 38.19% for the baseline model. The baseline model always predicted the first anomaly considerably ahead of time. Detecting anomalies too early could imply a risk of them being actual false positives. We hypothesize this is caused due to the domain shift and the baseline models actually mistaking different operational conditions as anomalies.

The results show the advantage of using transfer learning, due to two key advantages: allowing to reuse previously collected data, and modifying the model to perform under new conditions. It was demonstrated that using only the target domain data was not sufficient for detecting anomalies, and that using only the source domain data yielded models that were too sensible to the operating condition changes. These findings support the adoption of transfer learning techniques for bearing condition monitoring, enabling earlier detection of anomalies and allowing to reuse previously collected data.

ACKNOWLEDGMENTS

The authors would like to thank Bram Robberechts for performing the tests within the Smart Maintenance Living Lab project. *Funding* This work was supported by the Flemish Government under the "Onderzoeksprogramma Artificiële Intelligentie (AI) Vlaanderen" programme and the VLAIO subsidies for research.

Conflict of interest The authors declare no conflict of interest. The funders had no role in the design of the study; in the collection, analyses, or interpretation of data; in the writing of the manuscript, or in the decision to publish the results.

References

[1] Ooijevaar, T. H., Pichler, K., Di, Y., Devos, S., Volckaert, B., Van Hoecke, S., and Hesch, C. IFAC-PapersOnLine. Elsevier B.V., Amsterdam, The Netherlands, (2019). Smart machine maintenance enabled by a condition monitoring living lab, Vol. 52 376–381.

[2] Heng, A., Zhang, S., Tan, A. C., and Mathew, J. Rotating machinery prognostics: State of the art, challenges and opportunities. *Mechanical Systems and Signal Processing*. **23**, (3). (2009).

[3] Jardine, A. K., Lin, D., and Banjevic, D. A review on machinery diagnostics and prognostics implementing condition-based maintenance. *Mechanical Systems and Signal Processing*. **20**, (7). (2006).

[4] Yosinski, J., Clune, J., Bengio, Y., and Lipson, H. How transferable are features in deep neural networks? *Advances in Neural Information Processing Systems (NIPS)*. **27**. (2014).

[5] Zhang, R., Peng, Z., Wu, L., Yao, B., and Guan, Y. Fault diagnosis from raw sensor data using deep neural networks considering temporal coherence. *Sensors (Switzerland)*. **17**, (3). (2017).

[6] Kong, Y., Qin, Z., Han, Q., Wang, T., and Chu, F. Enhanced dictionary learning based sparse classification approach with applications to planetary bearing fault diagnosis. *Applied Acoustics*. **196**. (2022).

[7] Gebraeel, N., Lawley, M., Liu, R., and Parmeshwaran, V. Residual life predictions from vibration-based degradation signals: A neural network approach. *IEEE Transactions on Industrial Electronics*. **51**, (3). (2004).

[8] Huang, R., Xi, L., Li, X., Richard Liu, C., Qiu, H., and Lee, J. Residual life predictions for ball bearings based on self-organizing map and back propagation neural network methods. *Mechanical Systems and Signal Processing*. **21**, (1). (2007).

[9] Serradilla, O., Zugasti, E., Rodriguez, J., and Zurutuza, U. Deep learning models for predictive maintenance: a survey, comparison, challenges and prospects. *Applied Intelligence*. **52**, (10). (2022).

[10] Guo, L., Lei, Y., Xing, S., Yan, T., and Li, N. Deep Convolutional Transfer Learning Network: A New Method for Intelligent Fault Diagnosis of Machines with Unlabeled Data. *IEEE Transactions on Industrial Electronics*. **66**, (9). (2019).

[11] Liu, L., Wang, L., and Yu, Z. Remaining Useful Life Estimation of Aircraft Engines Based on Deep Convolution Neural Network and LightGBM Combination Model. *International Journal of Computational Intelligence Systems*. **14**, (1). (2021).

[12] Xia, M., Li, T., Xu, L., Liu, L., and De Silva, C. W. Fault Diagnosis for Rotating Machinery Using Multiple Sensors and Convolutional Neural Networks. *IEEE/ASME Transactions on Mechatronics*. **23**, (1). (2018).

[13] Eren, L., Ince, T., and Kiranyaz, S. A Generic Intelligent Bearing Fault Diagnosis System Using Compact Adaptive 1D CNN Classifier. *Journal of Signal Processing Systems*. **91**, (2). (2019).

[14] Sateesh Babu, G., Zhao, P., and Li, X.-L. Deep convolutional neural network based regression approach for estimation of remaining useful life. *Database Systems for Advanced Applications*. (2016).

[15] Wen, L., Li, X., Gao, L., and Zhang, Y. A New Convolutional Neural Network-Based Data-Driven Fault Diagnosis Method. *IEEE Transactions on Industrial Electronics*. **65**, (7). (2018).

[16] Hemmer, M., Van Khang, H., Robbersmyr, K., Waag, T., and Meyer, T. Fault Classification of Axial and Radial Roller Bearings Using Transfer Learning through a Pretrained Convolutional Neural Network. *Designs*. **2**, (4). (2018).

[17] Li, S., Liu, G., Tang, X., Lu, J., and Hu, J. An Ensemble Deep Convolutional Neural Network Model with Improved D-S Evidence Fusion for Bearing Fault Diagnosis. *Sensors*. **17**, (8). (2017).

[18] Xu, G., Liu, M., Jiang, Z., Söffker, D., and Shen, W. Bearing Fault Diagnosis Method Based on Deep Convolutional Neural Network and Random Forest Ensemble Learning. *Sensors*. **19**, (5). (2019).

[19] Chen, R., Huang, X., Yang, L., Xu, X., Zhang, X., and Zhang, Y. Intelligent fault diagnosis method of planetary gearboxes based on convolution neural network and discrete wavelet transform. *Computers in Industry*. **106**. (2019).

[20] Yoo, Y. and Baek, J.-G. A Novel Image Feature for the Remaining Useful Lifetime Prediction of Bearings Based on Continuous Wavelet Transform and Convolutional Neural Network. *Applied Sciences*. **8**, (7). (2018).

[21] Zhang, K., Tang, B., Deng, L., and Liu, X. A hybrid attention improved ResNet based fault diagnosis method of wind turbines gearbox. *Measurement*. **179**. (2021).

[22] Zhao, M., Kang, M., Tang, B., and Pecht, M. Deep Residual Networks with Dynamically Weighted Wavelet Coefficients for Fault Diagnosis of Planetary Gearboxes. *IEEE Transactions on Industrial Electronics*. **65**, (5). (2018).

[23] Kraus, M. and Feuerriegel, S. Forecasting remaining useful life: Interpretable deep learning approach via variational Bayesian inferences. *Decision Support Systems*. **125**. (2019).

[24] Lee, J., Lee, Y. C., and Kim, J. T. Fault detection based on one-class deep learning for manufacturing applications limited to an imbalanced database. *Journal of Manufacturing Systems*. **57**. (2020).

[25] Li, M., Yu, D., Chen, Z., Xiahou, K., Ji, T., and Wu, Q. H. A Data-Driven Residual-Based Method for Fault Diagnosis and Isolation in Wind Turbines. *IEEE Transactions on Sustainable Energy*. **10**, (2). (2019).

[26] Wang, F., Liu, X., Deng, G., Yu, X., Li, H., and Han, Q. Remaining Life Prediction Method for Rolling Bearing Based on the Long Short-Term Memory Network. *Neural Processing Letters*. **50**, (3). (2019).

[27] Zhu, Y., Zhu, C., Tan, J., Tan, Y., and Rao, L. Anomaly detection and condition monitoring of wind turbine gearbox based on LSTM-FS and transfer learning. *Renewable Energy*. **189**. (2022).

[28] Wu, C., Feng, F., Wu, S., Jiang, P., and Wang, J. A method for constructing rolling bearing lifetime health indicator based on multi-scale convolutional neural networks. *Journal of the Brazilian Society of Mechanical Sciences and Engineering*. **41**, (11). (2019).

[29] Pinedo-Sánchez, L. A., Mercado Ravell, D. A., and Carballo Monsivais, C. A. Vibration analysis in bearings for failure prevention using CNN. *Journal of the Brazilian Society of Mechanical Sciences and Engineering*. **42**, (12). (2020).

[30] Marei, M., Zaatari, S. E., and Li, W. Transfer learning enabled convolutional neural networks for estimating health state of cutting tools. *Robotics and Computer-Integrated Manufacturing*. **71**. (2021).

[31] Ying, Z., Shu, L., Kizaki, T., Iwama, M., and Sugita, N. Hybrid Approach for Onsite Monitoring and Anomaly Detection of Cutting Tool Life. *Procedia CIRP*. **104**. (2021).

[32] Zhang, K., Tang, B., Deng, L., Tan, Q., and Yu, H. A fault diagnosis method for wind turbines gearbox based on adaptive loss weighted meta-ResNet under noisy labels. *Mechanical Systems and Signal Processing*. **161**. (2021).

[33] Guo, L., Li, N., Jia, F., Lei, Y., and Lin, J. A recurrent neural network based health indicator for remaining useful life prediction of bearings. *Neurocomputing*. **240**. (2017).

[34] He, K., Zhang, X., Ren, S., and Sun, J. Deep residual learning for image recognition. *Proceedings of the IEEE Computer Society Conference on Computer Vision and Pattern Recognition*. **25**. (2016).

[35] Szegedy, C., Vanhoucke, V., Ioffe, S., Shlens, J., and Wojna, Z. Rethinking the Inception Architecture for Computer Vision. (2016).

[36] Deng, J., Dong, W., Socher, R., Li, L.-J., Li, K., and Fei-Fei, L. 2009 IEEE Conference on Computer Vision and Pattern Recognition. Imagenet: A large-scale hierarchical image database, (2009) 248–255.

[37] Hong, F., Song, J., Meng, H., Rui, W., Fang, F., and Guangming, Z. A novel framework on intelligent detection for module defects of PV plant combining the visible and infrared images. *Solar Energy*. **236**. (2022).

[38] Lu, W., Liang, B., Cheng, Y., Meng, D., Member, S., and Yang, J. Deep Model Based Domain Adaptation for Fault Diagnosis. *IEEE Transactions on Industrial Electronics*. **64**, (3). (2017).

[39] Hu, Q., Si, X., Qin, A., Lv, Y., and Liu, M. Balanced Adaptation Regularization Based Transfer Learning for Unsupervised Cross-Domain Fault Diagnosis. *IEEE Sensors Journal*. **22**, (12). (2022).

[40] Michau, G. and Fink, O. Unsupervised transfer learning for anomaly detection: Application to complementary operating condition transfer. *Knowledge-Based Systems*. **216**. (2021).

[41] Rao, W., Qu, Y., Gao, L., Sun, X., Wu, Y., and Zhang, B. Transferable network with Siamese architecture for anomaly detection in hyperspectral images. *International Journal of Applied Earth Observation and Geoinformation*. **106**. (2022).

[42] Saenko, K., Kulis, B., Fritz, M., and Darrell, T. Lecture Notes in Computer Science, Ed. 2010, C. V. E. Springer Verlag, (2010), Adapting visual category models to new domains, Vol. 6314 213–226.

[43] Ramakrishnan, R., Nagabandi, B., Eusebio, J., Chakraborty, S., Venkateswara, H., and Panchanathan, S. Deep hashing network for unsupervised domain adaptation. *Domain Adaptation in Computer Vision with Deep Learning*. (2020).

[44] Li, D., Yang, Y., Song, Y.-Z., and Hospedales, T. M. Deeper, Broader and Artier Domain Generalization. *2017 IEEE International Conference on Computer Vision (ICCV)*. (2017).

[45] Nectoux, P., Gouriveau, R., Medjaher, K., Ramasso, E., Chebel-Morello, B., Zerhouni, N., and Varnier, C. Conference on Prognostics and Health Management. PRONOSTIA: An experimental platform for bearings accelerated degradation tests, (2012) 1–8.

[46] Lee, J., Qiu, H., Yu, G., Lin, J., and Rexnord Technical Services. *IMS, University of Cincinnati. "Bearing Data Set"*. NASA Ames Research Center, Moffett Field, CA, 2007.

[47] Nieves Avendano, D., Vandermoortele, N., Soete, C., Moens, P., Ompusunggu, A. P., Deschrijver, D., and Van Hoecke, S. A Semi-Supervised Approach with Monotonic Constraints for Improved Remaining Useful Life Estimation. *Sensors 2022, Vol. 22, Page 1590*. **22**, (4). (2022).

[48] Lecun, Y., Bottou, L., Bengio, Y., and Haffner, P. Gradient-based learning applied to document recognition. *Proceedings of the IEEE*. **86**, (11). (1998).

[49] Karen, S. and Andrew, Z. Very deep convolutional networks for large-scale image recognition. (2015).

[50] Hasanpour, S. H., Rouhani, M., Fayyaz, M., and Sabokrou, M. Lets keep it simple, using simple architectures to outperform deeper and more complex architectures. *arXiv preprint arXiv:1608.06037*. (2016).

[51] Han, S., Pool, J., Tran, J., and Dally, W. J. Proceedings of the 28th International Conference on Neural Information Processing Systems. MIT Press, Cambridge, MA, USA, (2015). Learning both weights and connections for efficient neural networks, Vol. 1 of *NIPS'15* 1135–1143.

[52] Li, H., Kadav, A., Durdanovic, I., Samet, H., and Graf, H. P. Pruning filters for efficient convnets. (2017).

[53] Chenzhuo, Z., Song, H., Huizi, M., and William J., D. Trained ternary quantization. (2017).

[54] Wang, C.-H., Huang, K.-Y., Yao, Y., Chen, J.-C., Shuai, H.-H., and Cheng, W.-H. Lightweight deep learning: An overview. *IEEE Consumer Electronics Magazine*. (2022).

[55] Iandola, F. N., Han, S., Moskewicz, M. W., Ashraf, K., Dally, W. J., and Keutzer, K. Squeezenet: Alexnet-level accuracy with 50x fewer parameters and <0.5mb model size. *arXiv:1602.07360*. (2016).

[56] Barret, Z., Vijay, V., Jonathon, S., and Quoc V., L. Learning transferable architectures for scalable image recognition. (2017).

[57] Howard, A., Zhu, M., Chen, B., Kalenichenko, D., Wang, W., Weyand, T., Andreetto, M., and Adam, H. Mobilenets: Efficient convolutional neural networks for mobile vision applications. (2017).

[58] Dong, N., Zhang, C., and Chen, H. Proceedings of TEPEN 2022, Eds. Zhang, H., Ji, Y., Liu, T., Sun, X., and Ball, A. D. Springer Nature Switzerland, Cham, Research on fault diagnosis method of rolling bearing based on mobilenet v2. (2023) 528–533.

[59] Yu, W. and Lv, P. An end-to-end intelligent fault diagnosis application for rolling bearing based on mobilenet. *IEEE Access*. **9**. (2021).

[60] Pham, M. T., Kim, J.-M., and Kim, C. H. Deep learning-based bearing fault diagnosis method for embedded systems. *Sensors*. **20**, (23). (2020).

[61] Guzmán-Torres, J. A., Morales-Rosales, L. A., Algredo-Badillo, I., Tinoco-Guerrero, G., Lobato-Báez, M., and Melchor-Barriga, J. O. Deep learning techniques for multi-class classification of asphalt damage based on hamburg-wheel tracking test results. *Case Studies in Construction Materials*. **19**. (2023).

[62] Kim, B., Yuvaraj, N., Park, H. W., Preethaa, K. S., Pandian, R. A., and Lee, D.-E. Investigation of steel frame damage based on computer vision and deep learning. *Automation in Construction*. **132**. (2021).

[63] Bianco, S., Cadène, R., Celona, L., and Napoletano, P. Benchmark analysis of representative deep neural network architectures. *IEEE Access*. **6**. (2018).

[64] Andrew, H., Mark, S., Grace, C., Liang-Chieh, C., Bo, C., Mingxing, T., Weijun, W., Yukun, Z., Ruoming, P., Vijay, V., Quoc V., L., and Hartwig, A. Searching for mobilenetv3. *arXiv:1905.02244*. (2019).

[65] Alfredo, C., Adam, P., and Eugenio, C. An analysis of deep neural network models for practical applications. *arXiv:1605.07678*. (2016).

[66] Moens, P., Bracke, V., Soete, C., Vanden Hautte, S., Nieves Avendano, D., Ooijevaar, T., Devos, S., Volckaert, B., and Van Hoecke, S. Scalable Fleet Monitoring and Visualization for Smart Machine Maintenance and Industrial IoT Applications. *Sensors*. **20**, (15). (2020).

[67] Sandler, M., Howard, A., Zhu, M., Zhmoginov, A., and Chen, L. C. MobileNetV2: Inverted Residuals and Linear Bottlenecks. *Proceedings of the IEEE Computer Society Conference on Computer Vision and Pattern Recognition*. (2018).

[68] Kornblith, S., Chen, T., Lee, H., and Norouzi, M. Why Do Better Loss Functions Lead to Less Transferable Features? *Advances in Neural Information Processing Systems*. **34**. (2021).

[69] Michau, G., Frusque, G., and Fink, O. Fully learnable deep wavelet transform for unsupervised monitoring of high-frequency time series. *Proceedings of the National Academy of Sciences*. **119**. (2022).

[70] Park, D. S., Chan, W., Zhang, Y., Chiu, C.-C., Zoph, B., Cubuk, E. D., and Le, Q. V. Specaugment: A simple data augmentation method for automatic speech recognition. *Interspeech 2019*. (2019).

[71] Ruan, D., Chen, X., Gühmann, C., and Yan, J. Improvement of generative adversarial network and its application in bearing fault diagnosis: A review. *Lubricants*. **11**, (2). (2023).

[72] Kimura, D., Chaudhury, S., Narita, M., Munawar, A., and Tachibana, R. 2020 IEEE Winter Conference on Applications of Computer Vision (WACV). Adversarial discriminative attention for robust anomaly detection, (2020) 2161–2170.

[73] Belton, N., Hagos, M. T., Lawlor, A., and Curran, K. M. Proceedings of the IEEE/CVF Conference on Computer Vision and Pattern Recognition (CVPR) Workshops. Fewsome: One-class few shot anomaly detection with siamese networks, (2023) 2977–2986.

[74] Serradilla, O., Zugasti, E., Ramirez de Okariz, J., Rodriguez, J., and Zurutuza, U. Adaptable and explainable predictive maintenance: Semi-supervised deep learning for anomaly detection and diagnosis in press machine data. *Applied Sciences*. **11**, (16). (2021).

[75] Mingxing, T. and Quoc V., L. Efficientnet: Rethinking model scaling for convolutional neural networks. *arXiv:1905.11946*. (2019).